Proceedings of the 2024 Virginia Tech
Mechanical Engineering Senior Capstone Exposition
VTMECAP-2024
April 26, 2024, Blacksburg, Virginia, USA

VTMECAP-2024 - [01]

ACTIVE ASSTIVE MOVEMENT EXOSKELETON: CAN AID IN MOVEMENT SPEED

Christian Mueth[1], DeAndre Thomas[1], Jaison Dasika[1], Cole Gala[1], Shuhan Liu[1], Joseph Fleenor[1], Alan Asbeck[2]

[1]Department of Mechanical Engineering, Virginia Tech, Blacksburg, VA
[2]Assistive Robotics Lab, Virginia Tech, Blacksburg, VA

ABSTRACT

If one wishes to immediately increase one's sprinting speed beyond which one's body is typically capable, there is very little one can do beyond minor running technique or breathing pattern adjustments. This is why Team 01 of the Virginia Tech Mechanical Engineering Capstone projects has worked to develop a powered assistive exoskeleton with the goal of effectively increasing the wearer's speed.

The exoskeleton that the team has built features two motors, one to actuate extension and flexion of the hip, and one to provide an impulse at the ground, both working together to encourage the user's forward motion. According to current publications, no exoskeletons use this actuation scheme to increase a wearer's maximum sprinting speed. The team hopes to increase the sprinters speed by 15%, an increase in top speed that no other existing exoskeleton can offer according to current publications.

Through experimentation and analysis, Team 01 has concluded that the exoskeleton is able to exert the appropriate amount of torque and force at the hips and feet respectively, while weighing less than the derived weight threshold[1]. While experimentation did not provide conclusive regarding the wearers maximum sprinting speed, the team is confident that given the appropriate controls the exoskeleton has potential to increase an able-bodied individual's speed by 10-15%.

Keywords: Exoskeleton, assistive, sprinting, active

NOMENCLATURE

ε	Efficiency
k	Stiffness
M	Moment
$M_{desired}$	Desired Moment
F	Force
$F_{measured}$	Measured Force
d	Distance
K_p	Proportional Gain
K_d	Derivative gain

1. INTRODUCTION

For centuries, people have been trying to run faster. Running is an integral part of human movement, and it is widely beneficial to be able to run at high speeds. In the case of law enforcement officers and military personnel, the ability to sprint at high speeds can mean the difference between life and death. Thus, the purpose of this research is to generate a powered exoskeleton design that can increase a user's top sprinting speed.

There is only one exosuit in current publications that has been found to increase a user's sprinting speed. The powered exosuit developed by researchers at the Chung Ang University [1] was found to increase 9 test subject's speeds by an average of 0.97% during a 200m dash, increasing one participant's speed by 3.4% (Table 1). This was done solely through actuating hip extension.

Sprint time	No-suit			Suit-on		
	0–200 m	0–100 m	100–200 m	0–200 m	0–100 m	100–200 m
Participant 1	31.43	16.07	15.36	31.35	15.22	16.13
Participant 2	34.00	16.33	17.67	32.93	15.95	16.97
Participant 3	32.02	15.92	16.10	30.39	14.78	15.60
Participant 4	36.84	18.18	18.65	33.44	16.41	17.03
Participant 5	30.95	15.10	15.85	31.57	14.92	16.65
Participant 6	32.36	15.52	16.85	31.59	14.95	16.64
Participant 7	31.26	15.02	16.24	30.68	14.74	15.94
Participant 8	39.02	18.85	20.17	36.98	17.46	19.52
Participant 9	27.25	13.07	14.18	27.44	13.52	13.92
Average	32.79	16.01	16.79	31.82	15.33	16.49
SEM	1.15	0.57	0.60	0.86	0.38	0.49

TABLE 1: SPRINT TIMES OF PARTICIPANTS IN A 200M SPRINT [1]

The main system level objective is to increase a sprinter's speed by 15%. In doing so, it is hoped that the system will obtain the Guinness World Record for the "fastest 100m dash in a powered exoskeleton", as well as the men's or women's

[1] The desired weight threshold that the team derived is 22 lbs

Guinness World Record for the 100-meter dash. This is to be accomplished by actuating motion in hip extension and flexion, and by applying an impulse at a sprinter's foot.

2. DESIGN REQUIREMENTS / MATERIALS

Below are the materials and methods that were used when constructing and testing this exoskeleton.

2.1 Design Requirements and Analysis

To achieve a 15% increase in the wearers speed, it was determined through extensive analysis that the exoskeleton must meet five main criteria:

1. The hip subsystem must provide a torque of 60 Nm at the hips.
   a. Said torque must be applied in the proper direction[2].
2. The foot subsystem must provide a force of 500 N at the feet.
   a. Said force must be applied in the proper direction[2].
3. All actuation schemes must be able to apply these torques and forces adhering to the proper timing.
4. The exoskeleton must allow for all normal ranges of motion one would expect when sprinting.
5. The entire system must weigh less than 10kg (22lbs.)

For an exoskeleton that can meet all five of these requirements, analysis indicates it will have the ability to increase the wearer's speed by 15%. The methods used to verify these requirements are detailed in section 3 and section 4.

To determine the key system requirements, background research was performed to identify the various factors that can increase sprinting speed. Among the most important factors were increases in hip torque and increases in foot force. To aid in analysis, public data from research papers was used to build a linear correlation for percentage increase in a runner's peak speed from a percentage increase in peak hip torque and peak foot force respectively (figure 2). Assuming a mass of 100kg (220lbs.) for a runner, it was determined that a peak added foot force of 500N and a peak added hip torque of 60Nm would increase a runner's speed by 15%.

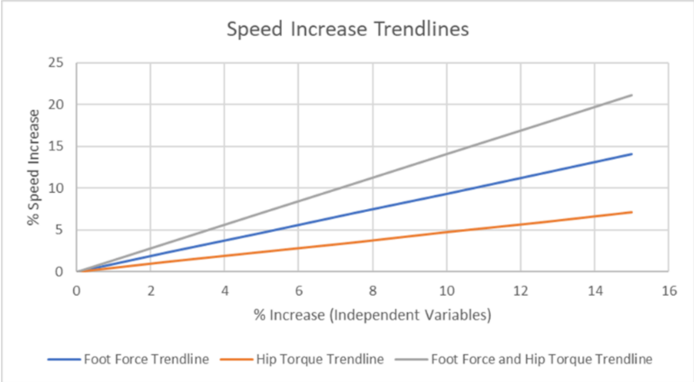

FIGURE 2: SPEED INCREASE TRENDLINES [2,3]

Following this, analysis was performed on how the system's added mass would affect the runner's speed. A trend was developed where percentage increases in the mass of the runner via pack loading were correlated with percentage decreases in speed (figure 3). This was accomplished using simple kinetic energy relations, where the peak kinetic energy of the runner without the added mass from pack loading was equated with the peak kinetic energy of the runner after pack loading. A pack loading of 10kg (22lbs.) was targeted. For a runner of 100kg (220lbs.) mass, this correlated with a 4% decrease in overall speed, allowing for a net speed increase of ~11%.

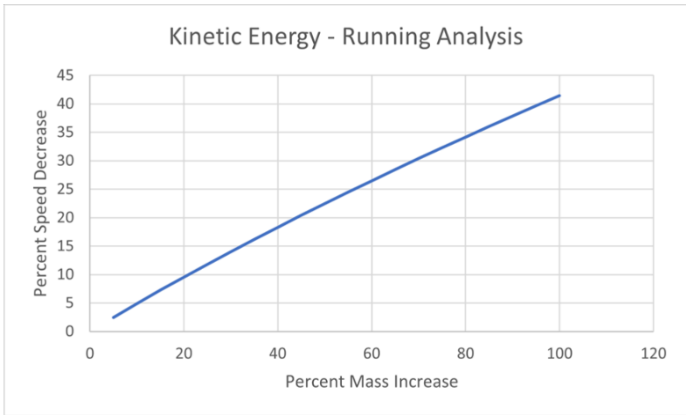

FIGURE 3: KINETIC ENERGY ANALYSIS PLOT

2.2 System Overview

The exoskeleton is divided into two subsystems, which will be referred to as the "hip subsystem" and "foot subsystem," respectively. Both systems work in parallel to assist the wearer in motion. Figure 4 shows the final exoskeleton in its entirety. The following sections detail how each system works with images of the systems CAD.

[2] The proper direction in this instance refers to such a direction that best encourages the wearer's forward motion

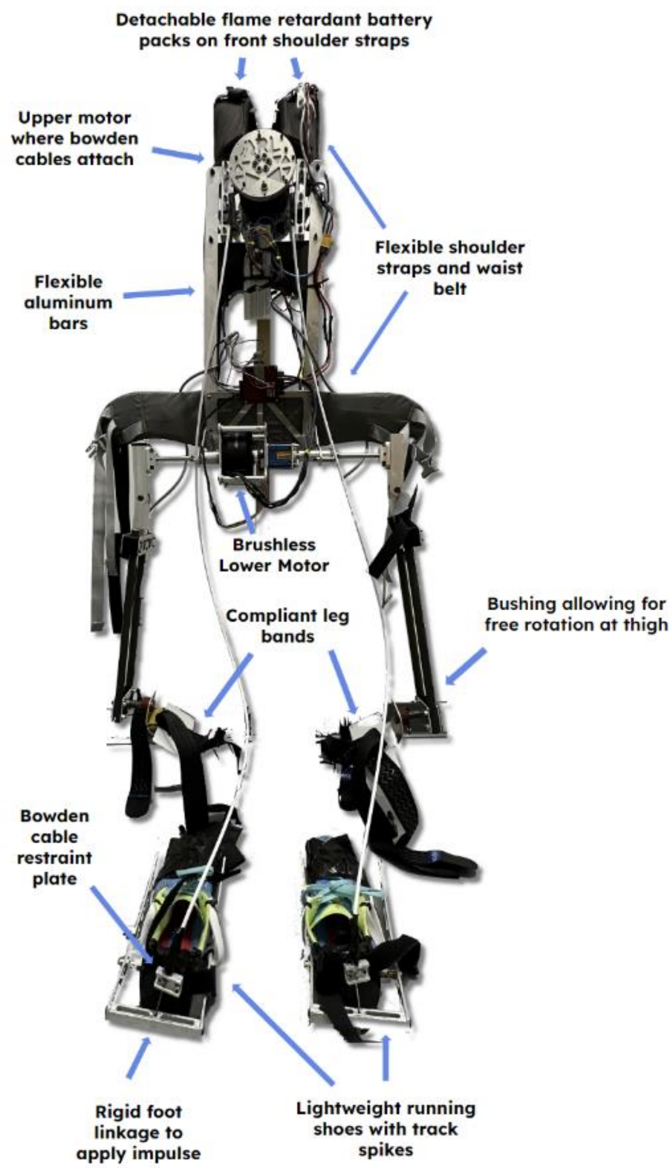

FIGURE 4: LABELED EXOSKELETON

2.3 Hip Subsystem - Mechanics

The hip subsystem actuates the hip through extension and flexion. The U13II motor, the primary actuator for this subsystem, exerts a force on the runner's thigh through a series of shafts and linkages.

The motor, seen in black on figure 5 encapsulated by a motor carriage, actuates when given power. It rotates a motor shaft through the input of an attached gearbox, which causes the entire system to rotate freely through two rotational bearings and about a rigid backplate. The motor can spin with respect to the motor carriage as well, effectively rotating the rightmost linkage (denoted as "square tubes" in figure 5) one direction while rotating the leftmost linkage the opposite direction. This motion essentially exerts a force on one leg, rotating that hip joint in flexion. Simultaneously, it exerts a force equal of equal and opposite magnitude on the opposite leg, rotating the opposite hip joint in extension.

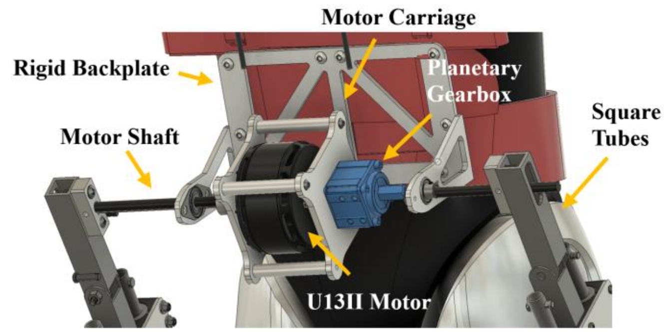

FIGURE 5: HIP ACTUATOR CAD MODEL

When the square tubes have a torque applied to them by the motor shaft, they rotate the leg by applying a force at the top of the thigh, using the rubber hoses as the point of contact (figure 6). They do this through a linear ball bearing pipe system. Two anodized aluminum tubes move linearly though a linear ball bearing system (highlighted blue in figure 6). This system is comprised of two linear ball bearings, held in place by black 3D printed PET-G retainers, sandwiched between two 2 mm (0.08 in) thick aluminum plates. Two aluminum plates of the same thickness are fastened to the ends of the anodized pipes as seen in the picture outlined in red in figure 6, with the shorter anodized pipe welded to the two plates.

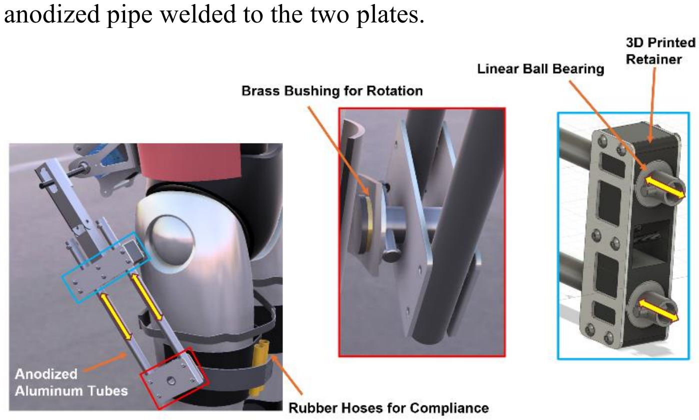

FIGURE 6: HIP MECHANICS CAD SCHEMATIC

This pipe can rotate freely about the brass bushing, secured with a clevis pin and a 3D printed retainer. The aluminum leg band then exerts a force on the rubber hoses, resulting compression or tension of the rubber hoses and exerting a force on the wearers thigh.

2.4 Hip Subsystem – Electronics and Controls

The U13II, a brushless DC outrunner motor designed for use in large agriculture drones, was selected due to its high power-to-weight ratio. The motor was controlled via an ODrive Pro motor controller, which allows for position, velocity, and force control for BLDC motors. A CUI quadrature motor encoder with incremental indexing is required for closed loop control with the ODrive as seen below in figure 7.

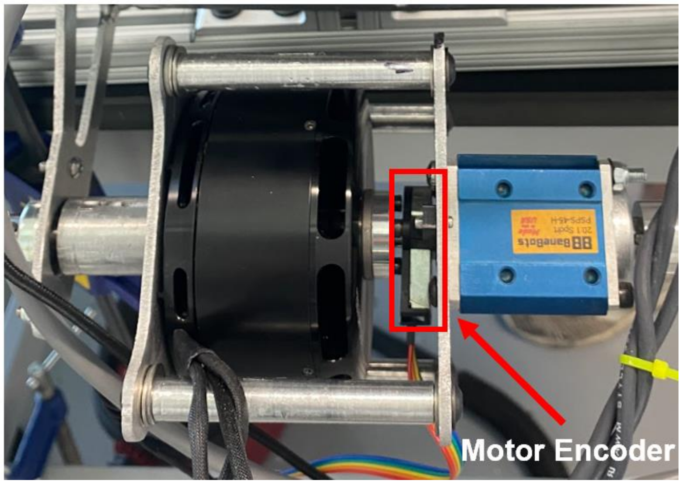

FIGURE 7: MOTOR ENCODER VISUAL

An ESP32 Feather Dev-Board microcontroller communicates with the ODrive Pro, sending signals dictated by the sensor data from two GY-521 MPU-6050 IMU's and a motor encoder that indicates the motor shaft's angular position.

The IMUs are secured with small 3D printed housings and a Velcro backing, attaching onto the leg band at the back of the user's thigh as seen in figure 8 below. This placement ensures optimal control data collection from the user's motion. This data is then sent to the ESP32 through I2C communication protocol using SCL and SDA pins. The AD0 pin for the first IMU is connected to the VCC pin. The second IMU has AD0 connected to the GND pin. This distinguishes the IMU addresses, giving the first IMU an address of 0X68 and the second IMU an address of 0X69 (the foot subsystem also utilizes this IMU wiring).

Additionally, a wireless remote was utilized to act as a "dead man's switch" where the user must continually hold down the switch to keep the system engaged. This remote was also used to proportionally control the motor's speed during testing. The remote was used in the early stages of testing in place of IMU control to control the motor without having to rely on complicated IMU controls.

FIGURE 8: IMU VISUAL

The hip and foot subsystem are powered by two Lumenier N2O Extreme 1550mAh 6s 150c LiPo batteries, which when connected in series supply 48 volts. These batteries power the U13II motor, the ODrive Pro, and the AK10-9 motor (see section 2.6).

A custom ESP32 program written in C++ controlled the U13II motor. This script took data from both IMUs and the wireless remote to send a corresponding velocity value to the ODrive Pro. The ESP32 is equipped with a WiFi transceiver, allowing for the microcontroller to host a local web server. This enabled connection to the ESP32's local network via a web browser to view a webpage that presented live telemetry data. The data presented included: battery voltage, motor speed, motor current, and any error codes that the ODrive threw. This webpage was crucial in being able to diagnose errors while the exoskeleton's wearer could be completely untethered (see section 3.4).

2.5 Foot Subsystem – Mechanics

To minimize mass and maximize range of motion for the foot subsystem, it was decided that force would be transmitted to the foot through Bowden cables which travel along plastic sheaths. Bowden cable actuation would be controlled via an oscillating motorized pulley, attached at the upper-back of the user (figure 9). The user also was to wear shoes featuring two aluminum linkages, which would pivot along a fulcrum. The fulcrum was installed into the shoe's rubber sole, normal to the foot. Bowden cables attached to the back of the aluminum linkages at the wearer's heel. When the cable was actuated upward, the linkage's fulcrum caused a force couple to be generated into the ground for an assistive ground reaction (figure 9).

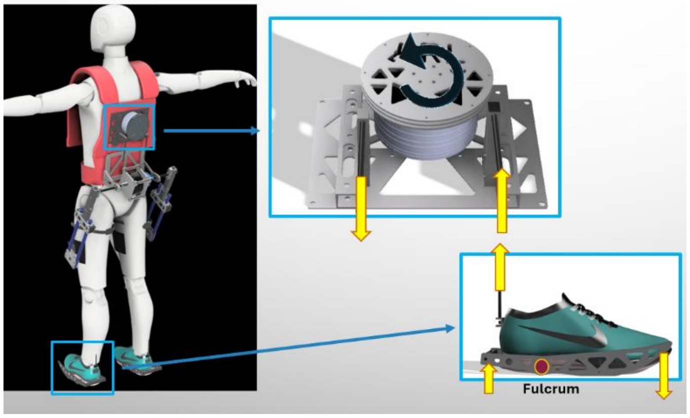

FIGURE 9: FOOT SYSTEM CAD SCHEMATIC

With the selection of Bowden cables, background research was performed on the force that could be transmitted for deflection of the cable. Using the assumption of a 5 cm (2 in) radius pulley and a 45-degree angle of oscillation, a deflection of 4 cm (1.57 in) was predicted for the Bowden cable system. Using a stiffness k of 25000 N/m from exoskeleton research data for Bowden cables [4], it was determined that the force transmitted to the user would be 1000N. A standard commercial efficiency ε of 70% was also assumed for the Bowden cables. Furthermore, an additional 70% efficiency factor was assumed due to a 45-degree angle when attaching to the foot linkage. Compounding these efficiencies, the overall efficiency of the Bowden cable system was predicted at 50%. Thus, the total force transmitted to the user was predicted to be the desired 500N. The AK10-9 motor was selected for actuation, due to speed-torque ratings allowing it to meet force requirements for the given pulley radius (see section 2.6).

Following this, research was performed on a variety of shoes. It was decided that the shoe for the system should feature carbon-fiber reinforcement, track-spikes, and be extremely lightweight. A carbon-fiber reinforced shoe helped ensure that the shoe would maintain structural integrity, even after installation of a mechanical fulcrum. Furthermore, background research suggested that carbon-fiber shoes boosted the general performance of runners [5]. Track spikes were also to be included, due to track-spikes being standard in optimal sprinting shoes.

A lightweight shoe of mass 0.21kg (0.46lbs.) was selected, which featured track-spikes and carbon-fiber reinforcement. Mechanical linkages were designed to this shoe, verified within 1.5 FOS for anticipated forces. After mechanical installations, the final shoe was weighed at 0.36kg (0.79lbs.), for an added mass of 0.15kg (0.33lbs.). To determine what the effect of added mass would be on sprinting speed, the required maximum torque to compensate for added mass needed to be identified. Inverse kinematics were performed using real-time angular acceleration and angular velocity data from a sprinter. This real-time data was collected using angles at a sprinter's hip, knee, and foot from a video by Texas Christian University [6], with the software Kinovea. From this, it was found that a peak torque of 10Nm would be required to compensate for added mass of 0.15kg at the feet. Correlating this peak compensating torque value with user speed, it was determined that the added mass to the shoe would reduce speed of the user by only ~1%.

Combining a 15% speed boost from increases in peak torque and peak force (section 2.1), a 4% speed reduction due to pack-loading (section 2.1), and a 1% speed reduction due to mass at the feet led to a theoretical net speed increase of ~10% from the system.

2.6 Foot Subsystem – Electronics and Controls

The foot subsystem's electronics (figure 10), include an ESP32 microcontroller and two IMU sensors (as described in section 2.4), which were validated to operate at speeds required for the foot subsystem. The electronics also feature a CAN bus driver, which communicates with an AK10-9 V2.0 6-8S brushless DC motor. The microcontroller and the IMU sensors receive power from the ODrive Pro in the hip subsystem (described in section 2.4), which provides a 5V voltage. The CAN bus driver facilitates CAN communication between the ESP32's GPIO pins and the motor.

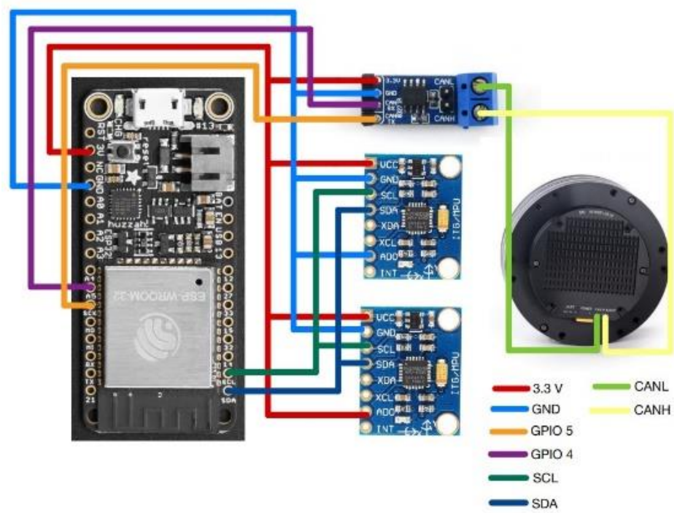

FIGURE 10: FOOT SYSTEM WIRING DIAGRAM

The AK10-9 motor for the foot subsystem is connected to two LiPo batteries for power (described in section 2.4). A C++ Arduino script was written using position control methods to actuate the motor. The motor starts at neutral position. To lift the left foot, the motor rotates 45-degrees clockwise and returns to neutral position. Similarly, to lift the right foot, the motor rotates 45-degrees counterclockwise and returns to neutral position.

The AK10-9 is a motor designed for usage in exoskeleton applications, but extensive motor analysis had to be performed to ensure that the motor could actuate within the required time-steps. Proportional-Derivative (PD) control was also utilized and tuned for the motor's position control (see sections 3.6 and 4.2). This allowed for proportional and compliant behavior with user biomechanics.

3. TESTING METHODS

A variety of tests were performed to determine if the exoskeleton would meet design requirement criteria. Tests were performed carefully and often multiple times, ensuring an accurate validation of design requirements.

3.1 System Weight Testing Methods

The system in its entirety was weighed to determine if it met design requirement 5: the system must weigh less than 10kg (22 lbs.). To do this, the following steps were performed:

1. The system was assembled in its entirety, with batteries equipped.
2. A force gauge was hooked to one of the straps at the top of the system.
3. The system was removed from its holding rack, being suspended in the air by the force gauge.
4. The readout of the force gauge was recorded as the system weight.

This process was performed for the foot and hip subsystems independently first, with each's weight recorded (figure 11). Then, the two subsystems were weighed together, ensuring an accurate weight for the entire system.

FIGURE 11: HIP SUBSYSTEM WEIGHING TEST

3.2 Range of Motion Testing Methods

Testing was performed to determine the wearer's range of motion when equipped with the exoskeleton. The range of motion requirements when sprinting were chosen as follows:

1. The ankle must be allowed to:
   a. Move through its entire range of dorsiflexion and plantarflexion.
   b. Medially and laterally rotate 5°-10°
2. The hip must be allowed to:
   a. Move 120° in flexion, keeping the shin perpendicular to the ground.
   b. Move 40° in extension, keeping the knee slightly bent.
   c. Move 5°-10° in both abduction and adduction.
3. The knee must be allowed to move in its full flexion and extension ranges of motion.
4. The shoulders must be allowed to move in their full ranges of motion.
5. The elbows must be allowed to move in their full flexion and extension ranges of motion.
6. The neck must be allowed to move 30° in extension and fully in flexion.
7. The lower back must be allowed to:
   a. Move in extension 5°-10°
   b. Move in flexion 30°-45°

These values were chosen given extensive analysis of normal ranges of motion when sprinting, and due to safety considerations when operating the exoskeleton.

Testing was performed as follows:

1. A person was equipped with the exoskeleton in its entirety and fastened to it securely.
2. With the system powered off, body parts were moved through the required ranges of motion. Required ranges of motion were exceeded when possible.
3. Range of motion tests were repeated multiple times, to ensure accuracy.

3.3 Hip Subsystem Testing Methods – Torque Testing

The first test that was conducted for the hip subsystem's actuation was testing whether the motor could supply the necessary amount of torque. To do this, the system was secured as illustrated in figure 12 below.

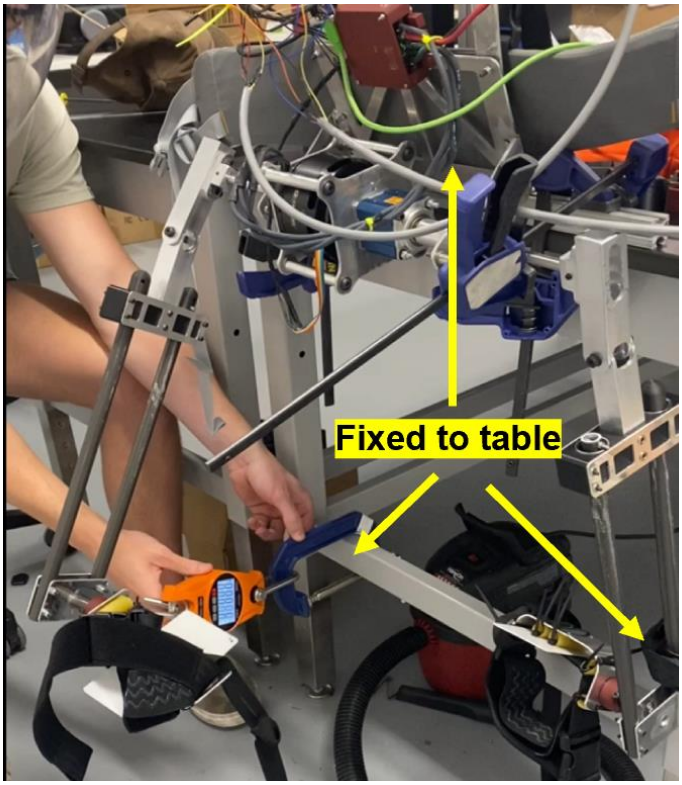

FIGURE 12: TORQUE TESTING SETUP

The two shoulder straps were secured to the 80-20 beams at the top of the exoskeleton, the rigid back plate and waistbelt were secured to the base of the table, and the leftmost hip linkage was secured to the table's leg. An orange force gauge was connected to a clamp, which was secured to the table, with the other end of the force gauge being secured to the lower portion of the rightmost hip linkage at approximately a 90° angle as seen in figure 13 below.

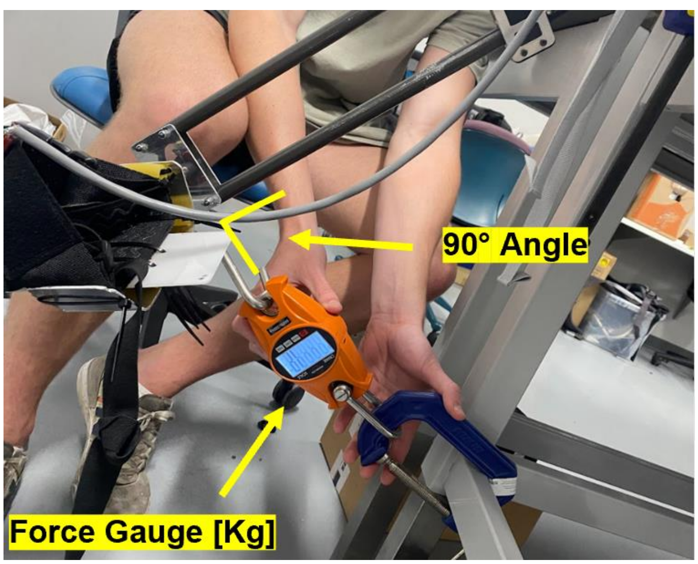

FIGURE 13: FORCE GAUGE SETUP

After setting this up, the motor was given power, and slowly actuated, supplying current to the motor at increments of 2 A. If the required force readout from the force gauge was calculated for a desired 60 Nm of torque at the hip in equation 1 as follows:

$$M_{desired}\ [Nm] = F_{measured}\ [N] * d\ [m] \tag{1}$$

$$F_{measured}\ [N] = \frac{M}{d} = \frac{60\ Nm}{0.5\ m} = 120\ N$$

$$120\ N\ * \ \frac{1\ kgf}{9.81\ N} = \mathbf{12.2\ kgf}$$

Current was supplied and increased until a readout of 12.2kg-f was recorded from the force gauge.

3.4 Hip Subsystem Testing Methods – Controls Testing

Once the previous three tests were performed, the controls for the system could be implemented. Essentially the testing plan was to ensure the team could receive data from the IMUs to influence the speed at which the motor ran, effectively actuating the exoskeleton using only human biomechanics.

First, the wearer was equipped with the exoskeleton on solid ground as opposed to the treadmill. Then the user began to move a leg in hip flexion, effectively moving the IMU, and data was collected on the motor characteristics on a web monitoring interface (as seen in figure 14).

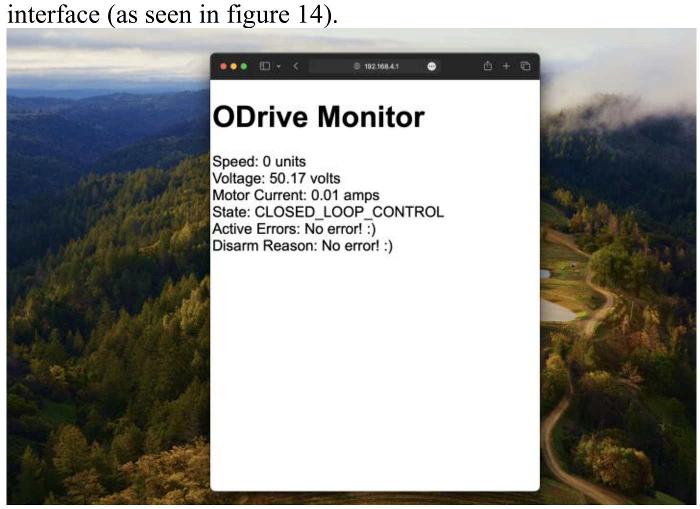

FIGURE 14: MOTOR MONITERING OUTPUT

It was then observed whether the motor actuated and "lifted" the leg up when in flexion. This was repeated for both legs, in both extension and in flexion.

Walking testing was then performed in a similar fashion, with the intent being to perform testing all the way up to sprinting on a treadmill.

3.5 Foot Subsystem Testing Methods – Force Testing

The foot system needed to be validated for generating forces of 500N via a force gauge. To test this, a user was equipped with the foot subsystem. Their shoe was then situated onto an aluminum block at the ground. The aluminum block allowed for the shoe's linkages to actuate into the air, with the user isolated from any forces. A force gauge was then secured to a fixed platform above the user, and cables were attached from the force gauge to the foot linkages (figure 15). The cabling system was adjusted to be held in tension, and the force gauge was canceled to remove any unwanted forces.

The current of the motor was steadily increased increments of 0.5A, causing corresponding increments in force to be output by the force gauge. Current and force gauge data from three tests were collected and built into trendlines. Linear equations from these trendlines were then used to map the maximum allowable current rating of the motor to a maximum allowable force output of the system. Finally, this maximum allowable force was compared with the required force to be output by the exoskeleton system.

FIGURE 15: FOOT SUBSYSTEM FORCE TEST SETUP

3.6 Foot Subsystem Testing Methods – Controls Testing

Controls for the foot subsystem also needed to be tested and implemented. To aid in this process, several different gait cycle tests were performed with the user wearing the foot subsystem on the treadmill. All tests on the treadmill began at walking gait speeds of 2mph and steadily increased to jogging gait speeds of 5mph.

For the first round of testing, IMU data was collected from both legs of the user. IMU data from the accelerometer axes and gyroscope axes were studied for consistent patterns, noise levels, and reliability. Once the best IMU sensor on each leg was determined, the sensor was to be implemented into a state-machine.

The state-machine using sensor data was to serial-print whether a user achieved a heel-strike states on the right leg or left leg during a gait cycle. Thus, once the IMU sensor state-machine was built, a second round of testing had to be performed on the treadmill. Footage was taken during treadmill tests, to compare a user's gait cycle with the state-machine's serial-print data. The state-machine was to be validated for speed and accuracy.

Following this, the AK10-9 motor was tuned using position control, with special attention given to K_p and K_d values characterizing the motor's PD loop. The motor's motions were to be validated for proportional, compliant, and reliable behavior.

Motor control was then folded into the sensor state-machine, and a final round of testing was performed on the treadmill. Slow-motion footage was taken, and the system was to be validated for whether it properly actuated during heel-strike for the right and left legs.

4. RESULTS AND DISCUSSION

Below detail the results of the tests performed, and conclusions drawn from those results.

4.1 Experimental Results – Entire System

Regarding system weight and the ranges of motion that the system can accommodate, the system satisfied the desired outcomes of these tests.

The system was found to weigh 9.6kg (21.16lbs.) in its entirety. With both the hip and foot subsystems being weighed independently, the foot system was found to weigh 4.2kg (9.26lbs.), and the hip system was found to weigh 6.1kg (13.45lbs.), each with a redundant mass of 0.7kg (1.5lbs.). With the two systems integrated and the redundant mass eliminated, the whole system was confirmed as weighing 9.59kg (21.16lbs.), which falls below the threshold of 10kg (22lbs).

The system in its entirety was also found to accommodate all the desired ranges of motion, as detailed in section 3.2 "Range of Motion Testing". Furthermore, the exoskeleton can accommodate a wider range of motion than required for many of the wearer's joints. A wide range of motion is a positive attribute of the system.

4.2 Experimental Results – Foot Subsystem

For tests validating that the motor could supply the appropriate force to the user, clear linear trendlines and linear equations were found across all three tests (figure 16). The maximum current rating of ~30A for the AK10-9 was then plugged into the linear equations for current-to-force.

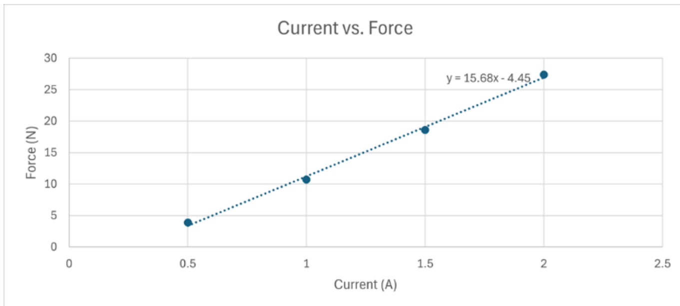

FIGURE 16: CURRENT VS. FORCE RESULTS

Across all three trials, the maximum force supplied by the motor was estimated at 500N, agreeing with early predictions. Furthermore, the maximum efficiency of the Bowden cable system was estimated at 50%, which also aligned with early predictions. Thus, major foot force requirements were met by the system. That said, there may still be ways to improve force output, via better management of Bowden cable bends and angles.

Gait cycle data from the IMUs revealed that angular velocity across the x-axes of the gyroscopes were the most reliable. Key thresholds from this data were identified and implemented into the system state machine (figure 17). The state machine was observed to reliably serial-print whether a user had made heel-strike with their left leg or their right leg.

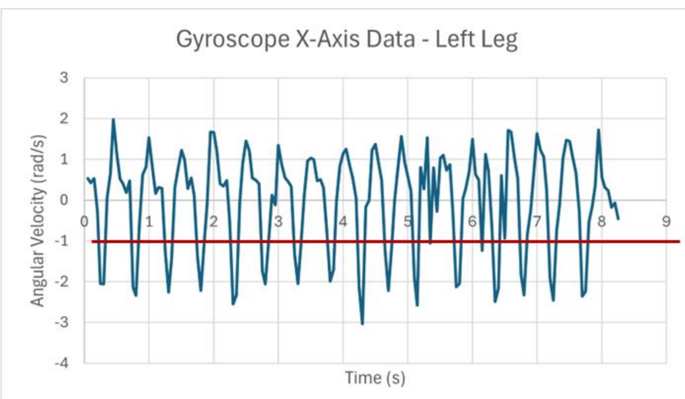

FIGURE 17: GYROSCOPE DATA

Motor tuning saw the motor exhibiting the required behaviors to assist in biomechanics. Motor control was then folded into the system state machine, and it was validated that the state-machine would reliably apply actuation during heel-strike for a user. Actuation was also observed assisting the user's biomechanics through their gait cycle (Figure 18).

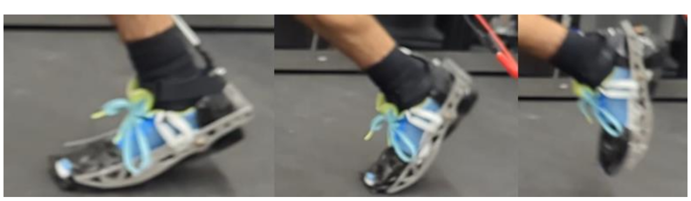
FIGURE 18: FOOT LINKAGE ACTUATION

Actuation testing worked up to jogging speeds of 5mph. More tuning of the motor's PD loop would be required for the exoskeleton to optimally boost a user while jogging or running.

4.3 Experimental Results – Hip Subsystem

The results of the torque testing (described in section 3.3) are as follows: it was found that the system can provide the necessary 60Nm of torque. A force readout of 15kg-f was recorded on the force gauge. A higher readout than the necessary 12.2kg-f was desired due to any error in the 90° angle of the force gauge and the rightmost linkage, as well as any other human error involved. The team is confident the motor is more than powerful for its needs. The recorded current that corresponded to this force reading was ~20A, which is only one third of the possible current that this motor can draw.

As for the controls for the hip system, IMU communication was successfully implemented for motor control. This was tested only as proof-of-concept, with the test subject standing still and simply actuating their leg through flexion. This was done using position control for the IMU. This control scheme is not viable for high-speed testing. However, a working controls scheme was identified and must be implemented to perform high speed testing.

Angular velocity control is to be used for the motor. Angular velocity commands derive from the angular velocity difference between a runner's legs, throughout a runner's gait cycle. This angular velocity difference would be determined using IMU gyroscope data, which would read the angular velocity from each leg.

Before the angular velocity difference data could be applied to the motor's output, a magnifying constant such as 1.1x or 1.5x would be applied. This would ensure the motor shaft applies a torque that rotates slightly faster than the wearers legs are rotating, properly propelling the runner forward. This controls scheme could ultimately allow for the hip subsystem to be tested at high speeds and be viable in increasing the runner's speed. This controls scheme was not implemented or tested due to time constraints (see section 4.4).

4.4 Comparison to Requirements

Given the results of the various tests, four out of the five design requirements for the system were met. The system can provide the desired torques in the desired directions, it can provide the desired forces in the desired directions, it weighs less than 10kg (22lbs.), and it allows for the appropriate ranges of motion. The only design requirement that this system failed to meet is requirement 3: "All actuation schemes must be able to apply these torques and forces adhering to the proper timing."

The main reason the system controls were not finished was the project's time-sensitive nature. Given only 8-9 months to design, model, fabricate, assemble, and test this exoskeleton, the team simply did not have enough time to implement the proper controls for the system. Thus, high speed testing could not safely be performed with the exoskeleton. Safe testing was only able to be performed for walking and jogging speeds, ranging from 2-5mph.

4.5 Technical Impact

While the exoskeleton failed to meet all the design criteria to increase a sprinters speed by 15%, the team believes the results of testing yielded significant impact on assisted movement. The exoskeleton possesses the mechanical ability to increase a wearer's sprinting speed, according to testing and analysis. It is believed that, given the right control scheme, the system could increase a sprinter's speed by at least 10%. Via testing results, it is also likely that this exoskeleton would be beneficial for assisted jogging or walking, allowing users to move while saving energy. Due to the system being powered, it can provide greater assistance than standard passive exoskeletons.

5. CONCLUSION

Ultimately, the team was unable to verify whether the exoskeleton can increase a sprinters speed by 15%. This was due to many reasons: miscommunication, long lead times during parts ordering, equipment malfunctions, and time-consuming controls required by the system. The team could not complete and refine its controls on time and thus could not conduct high-speed testing with the exoskeleton.

With that said, the exoskeleton mechanically aids one's motion at both low and high speeds according to analysis and testing. Given the proper control scheme, Team 01 is confident the system has the potential to increase a wearer's speed by at least 10%.

The insights that were gained when assembling and testing this exoskeleton were invaluable. Hopefully they will guide future iterations of the project to one day break the world record for the 100-meter dash.

ACKNOWLEDGEMENTS

Team 1 would like to thank the faculty and staff at the Virginia Tech Mechanical Engineering Department for providing the funding for this project, as well as for guidance and the other resources that were utilized.

Team 01 would like to thank Dr. Alan Asbeck for his numerous contributions to the design, assembly and testing of this exoskeleton, and the guidance and insight he provided. Team 01 is grateful to Dr. Asbeck and Virginia Tech for allowing work to be performed in the Assistive Robotics Lab at Virginia Tech, and for allowing use of its resources.

Thank you to Matthew Collins and the Applied Lab at Virginia Tech for assistance and resources when fabricating many of the components of the project.

REFERENCES

[1] Moon, J., Nam, K., Ryu, J., Kim, Y.-S., Yun, J., Yang, S., Yang, J., and Lee, G., 2023, "Reducing Sprint Time with Exosuit Assistance in the Real World," Zenodo (CERN European Organization for Nuclear Research).

[2] Weyand, P. G., Sandell, R. F., Prime, D. N. L., and Bundle, M. W., 2010, "The Biological Limits to Running Speed Are Imposed from the Ground Up," Journal of Applied Physiology, 108(4), pp. 950–961.

[3] Schache, A. G., Blanch, P., Dorn, T. W., Brown, N., Rosemond, D., and Pandy, M. G., 2011, "Effect of Running Speed on Lower Limb Joint Kinetics," Medicine and Science in Sports and Exercise, 43(7), pp. 1260–1271.

[4] Quinlivan, B., Asbeck, A. T., Wagner, D., Ranzani, T., Russo, S., and Walsh, C. J., 2015, *Force Transfer Characterization of a Soft Exosuit for Gait Assistance*, ASME 2015 International Design Engineering Technical Conferences.

[5] Gregory, R. W., Axtell, R. S., Robertson, M., and Lunn, W. R., 2018, "The Effects of a Carbon Fiber Shoe Insole on Athletic Performance in Collegiate Athletes," Journal of Sports Science, 6(4).

[6] Texas Christian University, 2014, "National Champion Sprinter at 26+ Mph on SMU Force Treadmill," YouTube.

[7] Bezodis, I., Kerwin, D. G., and Salo, A., 2008, "Lower-Limb Mechanics during the Support Phase of Maximum-Velocity Sprint Running," Medicine and Science in Sports and Exercise, 40(4), pp. 707–715.

[8] Weyand, P. G., Sternlight, D. B., Bellizzi, M. J., and Wright, S., 2000, "Faster Top Running Speeds Are Achieved with Greater Ground Forces Not More Rapid Leg Movements," Journal of Applied Physiology, 89(5), pp. 1991–1999.

[9] Asbeck, A. T., Schmidt, K., and Walsh, C. J., 2015, "Soft Exosuit for Hip Assistance," Robotics and Autonomous Systems, 73, pp. 102–110.

[10] Clark, K. P., and Weyand, P. G., 2014, "Are Running Speeds Maximized with Simple-Spring Stance Mechanics?," Journal of Applied Physiology, 117(6), pp. 604–615.

[11] Witte, K. A., Fiers, P., Sheets-Singer, A. L., and Collins, S. H., 2020, "Improving the Energy Economy of Human Running with Powered and Unpowered Ankle Exoskeleton Assistance," Science Robotics, 5(40).

[12] Boffey, D., Harat, I., Gepner, Y., Frosti, C. L., Funk, S., and Hoffman, J. R., 2018, "The Physiology and Biomechanics of Load Carriage Performance," Military Medicine, 184(1–2), pp. e83–e90.

[13] Chen, L., Chen, C., Ye, X., Wang, Z., Liu, Y., Cao, W., Chen, S., and Wang, X., 2022, "A Portable Waist-Loaded Soft Exosuit for Hip Flexion Assistance with Running," Micromachines, 13(2), p. 157.

[14] Kim, J.-S., Lee, G., Heimgartner, R., Revi, D. A., Karavas, N., Nathanson, D., Galiana, I., Eckert-Erdheim, A., Murphy, P. J., Perry, D., Menard, N., Choe, D. K., Malcolm, P., and Walsh, C. J., 2019, “Reducing the Metabolic Rate of Walking and Running with a Versatile, Portable Exosuit,” Science, 365(6454), pp. 668–672.